Published in final edited form as:
J Neurosci Methods. 2011 April 15; 197(1): 48–55. doi:10.1016/j.jneumeth.2011.01.029.

Autofluorescent cells in rat brain can be convincing impostors in green fluorescent reporter studies

Nadja Spitzer, **Gregory S. Sammons**, and **Elmer M. Price**
Department of Biological Sciences and Cell Differentiation and Development Center, Marshall University, Huntington, WV

Abstract

Cell transplant and gene therapies are promising approaches to many disorders of the nervous system. In studies involving cell transplants to the brain or nervous system, expression of green fluorescent protein (GFP) is commonly used to label cells, allowing their identification and histological assessment even after long post-operative survival times. Techniques employing viral tracing or reporter genes also commonly use GFP to label cells. Here, we document the presence of a subpopulation of green autofluorescent cells in the cortex and hippocampus of formaldehyde fixed, cryosectioned rat brains aged 3–9 months. Using standard microscopic fluorescence imaging techniques, we acquired clear images of green autofluorescent cells, complete with extensive processes, which appear to be well integrated into the host tissue. Treatment of brain sections with sodium borohydride followed by cupric sulfate in ammonium acetate buffer reduced background and cellular autofluorescence throughout sections but, especially in hippocampus, did not eliminate considerable green fluorescence in a subset of neurons. This autofluorescence was weak and would therefore pose a problem only when cells weakly express GFP or when few labeled cells survive. We suggest that investigators be aware of the potential for false positives, especially if the cells expressing GFP are expected to migrate widely from the transplant site. Parallel sections from naïve brains should regularly be processed and imaged alongside experimental brain sections, and anti-GFP immunohistochemistry should be performed to ensure that true GFP^+ signals are imaged instead of endogenous autofluorescent neurons.

Keywords

hippocampus; green fluorescent protein; cortex; false positive; cell therapy; viral vectors

1. Introduction

The fields of cell and gene therapy have exploded over recent decades and their application to disorders of the central nervous system has been the object of much study and clinical trials since the 1990s (reviewed in Lim et al., 2010; Serakinci and Keith, 2006; Sharp and Keirstead, 2009; Zietlow et al., 2008). Green fluorescent protein (GFP), or, more recently, enhanced GFP (eGFP), expression is an elegant and widely used method of identifying cells in tissues after transplant or gene therapy. These techniques harness the inherent

Corresponding author: Nadja Spitzer, Ph.D., Department of Biological Sciences, Marshall University, One John Marshall Dr., Huntington, WV, 25755, tel: 304.696.3778, fax: 304.696.3766, spitzern@marshall.edu.

fluorescence of the protein product from the GFP gene of the jellyfish, *Aequoria victoria* (Chalfie et al., 1994). Cells are stably transfected with the GFP gene, or are isolated from donor animals that are transgenic for GFP. After introduction into an experimental animal, the transplanted cells continue to produce GFP thus allowing investigators to identify transplanted cells even after extended periods of time (Shetty et al., 2008; Webber et al., 2007) or after active migration of cells away from the transplant site (Yamasaki et al., 2007).

Here we demonstrate that primarily hippocampus and sometimes cortex in normal rat brain cryosections from young animals contain a subpopulation of green autofluorescent neurons. These cells are distinctive and easily imaged, with reasonable exposure times, in epifluorescence microscopy with eGFP filter sets, when sections are processed using standard immunohistochemistry protocols. We test the efficacy of treating brain sections with sodium borohydride ($NaBH_4$), to reduce general background fluorescence caused by formaldehyde fixation (Clancy and Cauller, 1998), followed by cupric sulfate ($CuSO_4$), to quench lipofuscin autofluorescence (Schnell et al., 1999), in reducing the signal from the autofluorescent cells. Finally, we demonstrate that, when a true green fluorescent signal is present, the exposure times become sufficiently short, minimizing visualization of the autofluorescent cells. The technique of using green fluorescent labels is therefore not problematic as such, however, when few transplanted cells survive or if GFP expression is not stable, the endogenous autofluorescent cell population described here may be mistakenly identified as GFP-positive cells even after standard treatments to reduce autofluorescence.

2. Methods

2.1 Chemicals

Unless otherwise indicated, all chemicals were purchased from Sigma-Aldrich Corp., St. Louis, MO.

2.2 Animal subjects

Animal care and procedures were performed under an approved protocol from the Institutional Animal Care and Use Committee at Marshall University and conformed to National Institutes of Health guidelines. Sprague Dawley rats were obtained from Hilltop Lab Animals (Scottsdale, PA) and provided with rat chow and water *ad libitum*. We observed autofluorescent cells in brain sections from rats that were either completely naïve (n=7 of 20), received only a standard unilateral 6-hydroxydopamine (6-OHDA) lesion (15 μg delivered to medial forebrain bundle) to induce hemi-Parkinsonian symptoms (n=12 of 20) (Blandini et al., 2008; Ungerstedt, 1968) or received a sham saline injection to the striatum in addition to the 6-OHDA lesion (n=1 of 20). These treatments are commonly used as a model of Parkinson's disease and characterization of autofluorescence in these brains is especially relevant for investigators using GFP labeled cells in transplant therapies addressing this disease. In this study, only the side of the brain contralateral to the treatments was examined. Rats were sacrificed at ages from three to nine months old as specified in Table 1.

Animals were deeply anesthetized with 5% isofluorane, killed by bilateral pneumothorax, flushed with PBS (0.1 M, pH7.4) and perfusion fixed with 4% paraformaldehyde in PBS via cardiac puncture. The brain was recovered quickly by gross dissection of the dorsal surface of the skull; cranial nerves and olfactory bulbs were cut. Intact brains were post-fixed in 4% paraformaldehyde overnight and then moved to 30% sucrose in PBS at 4°C until no longer buoyant. Brains were blocked using a razor blade and mounted with Tissue-Tek OCT compound (Sakura Finetek, Torrance, CA), 30 μm sections were cut on a cryostat (Leica, Bannockburn, IL) and stored free floating in 48-well plates (Fisher Scientific, Pittsburgh,

PA) at −20°C in cryoprotectant (30% glycerol, 30% ethylene glycol, in PBS) until histochemical processing was conducted.

2.3 Histochemistry

Free floating tissue sections were transferred from cryoprotectant to mesh inserts (Corning, Lowell, MA) and washed four times 5 min in PBS. Sections were then incubated in fresh 1% $NaBH_4$ in PBS for 20 min. For immunohistochemistry, the sections were washed four times and then pre-blocked with 10% normal goat serum (NGS) in PBS containing 0.3% Triton X100 (PBTX) for 1 hr at room temperature followed by two PBS washes. Sections were incubated in PBTX containing 1% NGS and 1:500 primary antibodies overnight at 4°C. Primary antibodies were mouse anti-β-tubulin III, -NeuN and -glial fibrillary acidic protein (GFAP) (all from Millipore, Billerica, MA) and rabbit anti-5-HT (Immunostar, Hudson, WI). Sections were then washed four times in PBS and incubated in PBTX containing 1% NGS and secondary antibodies at 1:500 for 2 hrs followed by three PBS washes. Secondary antibodies were goat anti-mouse or goat anti-rabbit immunoglobulins conjugated to Alexa 568 or Alexa 488 (Invitrogen, Carlsbad, CA). Sections were then washed in PBS four times 5 min, rinsed in H_2O and incubated for 1 hr in 1 mM $CuSO_4$ in 50 mM ammonium acetate, pH5.0. After rinsing in H_2O, sections were washed four times 5 min in PBS with TO-PRO-3 iodide (1 μM, Invitrogen) or DAPI (10 μg/ml, Santa Cruz Biotechnology, Santa Cruz, CA) included in the last wash. As indicated, processing of some sections omitted the $NaBH_4$, immunohistochemistry, and/or $CuSO_4$ steps.

After the final wash, sections were mounted on Superfrost plus glass slides (Fisher) in H_2O, allowed to dry briefly and cover slipped with Prolong Gold (Invitrogen). After curing overnight, slides were stored at 4°C until imaging.

During our experimental design we tested a range of concentrations and exposure times for the $NaBH_4$ and $CuSO_4$ steps as described in the original papers (Clancy and Cauller, 1998; Schnell et al., 1999). We chose the parameters that gave the best reduction of autofluorescence and background fluorescence without compromising the brightness and clarity of specific immunohistochemical signals. Specifically, sections were incubated in fresh 1% $NaBH_4$ in PBS for 20 min before exposure to antibodies and 1 mM $CuSO_4$ in 50 mM ammonium acetate, pH5.0 for 1 hr after immunostaining.

2.4 Imaging

Epifluorescent light images were obtained with a Zeiss Axio Observer using 10× and 20× LD Plan Neofluar air-interface objectives (Zeiss, Jena, Germany). Green images were acquired using a 38HE filter set (for eGFP) from Zeiss (excitation BP 470/40; beam splitter FT 495; emission BP 525/50). Images were recorded with AxioVision 4.6.3 software using default settings for z-stack projections.

Confocal images were obtained with a BioRad/Zeiss MRC 1024 confocal scanning system (Zeiss) with inverted Nikon Diaphot 300 light microscope (Nikon Instruments Inc., Melville, NY) in Marshall University's imaging core facility. A Nikon PlanApo 20/0.75 air-interface objective was used and images were recorded with BioRad Lasersharp 2000 v5.2 software.

Brightness and contrast manipulations were applied uniformly to entire images using ImageJ (NIH, Bethesda, MD). Figures were constructed using Adobe Illustrator CS3 on a Macintosh computer.

3. Results

Rat brain sections that were simply washed in PBS and mounted exhibited extensive autofluorescence in the green channel (Figure 1A). This autofluorescence consisted of two separate signals; an overall diffuse fluorescence throughout the tissue and a punctate or granular signal localized primarily to somata. Autofluorescent cells were localized primarily to hippocampal and cortical regions with some cells visible throughout other brain regions such as striatum, amygdala, thalamus and olfactory bulb. Especially in and around the pyramidal cell layer of the CA regions in the hippocampus, autofluorescent cells were prominent, with cell bodies and extensive lengths of neurites visible using standard image acquisition parameters as detailed below (Figure 1A). Green autofluorescent cells were also often observed in the granular cell layer and hilus of the dentate gyrus and distributed throughout the hippocampus. Histochemical treatment of the brain sections with $NaBH_4$ (Clancy and Cauller, 1998) followed by $CuSO_4$ in ammonium acetate buffer (Schnell et al., 1999) dramatically reduced the intensity of the overall background fluorescence and the number and intensity of cells exhibiting the punctate fluorescent signal (Figure 1B). Hippocampus was the only brain region that consistently contained cells with prominent autofluorescent signals after these quenching treatments although some brains retained small numbers of autofluorescent cells in other brain regions, especially cortex. To characterize the properties of the autofluorescent signal, we applied each treatment separately. In untreated sections, endogenous autofluorescence appeared as an overall diffuse fluorescence that increased background and delineated some cells and their neurites in addition to a grainy or punctate signal localized primarily to somata in hippocampus, cortex (Figure 1C&G) and other regions. Treatment of serial sections with $NaBH_4$ reduced the overall diffuse fluorescence, resulting in fewer visible neurites, but leaving a prominent punctate signal in somata (Figure 1D&H). Conversely, the punctate signal was reduced by treatment with $CuSO_4$ but the diffuse signal was not affected (Figure 1E&I). By subjecting sections to treatment with $NaBH_4$ followed by $CuSO_4$, the autofluorescence in all brain areas was greatly reduced, however, the somata and neurites of some individual cells, especially in hippocampus, remained appreciably fluorescent and distinct from background (Figure 1F&J).

The cellular autofluorescence apparent in sections treated with $NaBH_4$ and $CuSO_4$ was most prominent in the green channel (Figure 2A; ex470/40, bs495, em525/50; 339 ms exposure), clearly delineating somata and neurites of hippocampal cells. Weak autofluorescent signals restricted to the brightest part of the signal in the somata could also be observed in the red (Figure 2B; ex572/25, bs590, em629/62, 730 ms exposure) and blue (Figure 2C; ex365/12, bs395, emLP397, 82 ms exposure) channels but were barely visible at the long red end of the spectrum (Figure 2D; ex620/60; bs660; em700/75; 453 ms exposure).

The autofluorescent cells visible after treatment with $NaBH_4$ and $CuSO_4$ represent a population of neurons, as they were immunoreactive for the standard neural markers NeuN and β-tubulin III (Figure 3). Confocal microscopy revealed that the green autofluorescent signals were localized to $NeuN^+$ or β-tubulin III^+ cells (Figure 3C& D). The cells did not label for glial fibrillary acidic protein (GFAP), a marker of astrocytes (data not shown). Immunohistochemistry for these markers underscored the fact that the green autofluorescent cells were surrounded by other neurons and incorporated in the brain parenchyma but unique in their green autofluorescent properties.

Numerous cells and fiber tracts throughout the brain were immunopositive for the biogenic amine, serotonin (5-HT), including extensive labeling in hippocampus (Figure $4A_1\&B_1$), but most of these cells were not inherently autofluorescent (Figure $4A_2\&B_2$). Conversely, only some green autofluorescent cells contained 5-HT (Figure $4A_4\&B_4$).

Prominent autofluorescent cells were observed after quenching with $NaBH_4$ and $CuSO_4$ in all 20 rat brains examined (Table 1). The animals ranged in age from young (3 months old) to adult (9 months old) with representative hippocampal autofluorescence after $NaBH_4$ and $CuSO_4$ treatments for the range of ages shown in Figure 5. The youngest animal in the group (3 months old, Figure 5A) had relatively few autofluorescent cells that were localized primarily to hippocampus. However, within the range of 4–9 months of age, the number and distribution of autofluorescent cells in treated sections did not qualitatively correlate with the animal's age. For example, the hippocampus from a 4 month old animal contained numerous autofluorescent cells with extensive processes (Figure 1A&B) as did the brains of 5,6 or 8 month old animals (Figure 5B,C,E). Conversely, a 7 month old brain contained relatively few autofluorescent cells (Figure 5D), although the brain from another 7 month old animal was rich in autofluorescent cells (Figure 1C–F). The high variability in autofluorescent cell numbers (Table 1) and the animals' limited age distribution in our data set (16 of 20 aged 5–7 months, one animal each at extremes of 3 months and 9 months old; Table 1) precludes more quantitative examination of age effects on autofluorescence. However, qualitative assessment (Figure 5; Table 1) suggests that there was little correlation between age and the size of the autofluorescent cell population.

Although the autofluorescent cells apparent after treatment with $NaBH_4$ and $CuSO_4$ were distinctive and could be visualized using standard image acquisition methods (see below), they are faint and do not interfere with the imaging of a robust green fluorescent signal when one is present. Green signals from autofluorescence and immunohistochemistry in the same tissue section could be distinguished by varying the image acquisition times. Hippocampal autofluorescent cells in untreated brain sections were imaged with an acquisition time of 384 ms (Figure 6A). A serial section from the same brain was treated with $NaBH_4$ and $CuSO_4$ and processed for immunohistochemistry to visualize GFAP using a green Alexa 488 secondary antibody (Figure 6B). In this section, the bright green fluorescence of the immunolabel could be captured using a shorter 93 ms exposure time, thus excluding visualization of the autofluorescent cells. This was supported by the lack of green signal in a serial section, processed in the same way but omitting the primary antibody, and imaged with a 93 ms exposure (Figure 6C). A longer exposure time, 384 ms, of the same field in the same section reveals underlying autofluorescent cells (Figure 6D).

4. Discussion

Survival, differentiation, and integration of transplanted cells into endogenous circuits are major challenges in cellular therapy of central nervous system disorders (Brederlau et al., 2006; Karlsson et al., 2005; Zeng et al., 2004). Specific populations of cells expressing GFP are becoming increasingly accessible and this label is commonly used to track transplanted cells in the nervous system. GFP is also commonly used as a reporter for viral tracking or expression of specific genes. However, our findings suggest that investigators must use caution when looking for transplanted GFP^+ cells in rat brain sections. This is especially true if those cells were transplanted to a region (e.g. ventricle or corpus callosum) or with a protocol (e.g. using guidance cues) such that extensive migration or dispersion of a limited number of green cells might be expected.

Here we show that normal and unlabeled rat brain sections contain a population of neurons that are sufficiently autofluorescent in the green channel (Ex 470/40 nm; Em 525/50 nm), even after chemical quenching, to generate convincing images using normal epifluorescence techniques and settings for imaging eGFP. Autofluorescence located to individual cells is widespread throughout hippocampus, cortex and other brain regions in formaldehyde fixed and cryosectioned brains, and can be significantly reduced by treating the sections with sodium borohydride ($NaBH_4$) followed by cupric sulfate ($CuSO_4$) in ammonium acetate

buffer. These treatments reduce general background fluorescence (Clancy and Cauller, 1998) and quench lipofuscin autofluorescence (Schnell et al., 1999), almost eliminating the problem in most brain regions. In hippocampus, however, a prominent subpopulation of autofluorescent cells consistently remains even after these treatments.

While it is expected that negative control sections omitting the primary antibody be processed in parallel when performing immunohistochemistry, it is less common to include sham surgery brains that did not receive a cellular transplant as a negative control in histochemistry of transplant studies. This is somewhat understandable, as one would not expect to find GFP^+ cells in a naïve brain. Indeed, there are no endogenous cells as bright as a strong green fluorescent signal in rat brain sections. However, if few of the transplanted cells survive, or if GFP^+ expression is unstable and variable (Kong et al., 2009), the weaker green signal of the endogenous autofluorescent cells described here will be clearly visible and may be mistaken for transplanted cells that have migrated to the hippocampus or cortex and incorporated extensively into the host tissue.

The localization of this population of autofluorescent cells to the hippocampus highlights this problem in the field of stem cell therapy for CNS disorders, especially stroke, epilepsy or Alzheimer's disease (Shetty et al., 2008). The hippocampus is one of the brain regions known for adult neurogenesis and is therefore likely to provide a hospitable environment for survival and differentiation of stem cells (Gage, 2000). Indeed, astrocytes isolated from the hippocampus stimulate neural differentiation in adult neural stem cells (Song et al., 2002). In addition, the development of long neurites, incorporation into brain tissue, and expression of neural markers are regularly used as indicators of survival and integration of transplanted cells. Because the autofluorescent cells described here are endogenous neurons, they will demonstrate all the structural, cellular and molecular attributes of a true, functional neuron and could lead to incorrect positive interpretation of a GFP^+ labeling study. When cells robustly expressing GFP are present, the autofluorescent cell population is not likely to interfere with data collection, because GFP^+ signals would be sufficiently bright to allow imaging settings that banish the autofluorescent cells to the background.

Because the hippocampus is famously one of the sites in the adult brain that continues to experience neurogenesis throughout adulthood (Eriksson et al., 1998; van Praag et al., 2002), it is tempting to speculate that the unique autofluorescent cells described here are different from their neighbors because they are newborn neurons. However, we did not consistently observe similar autofluorescent cells remaining after $NaBH_4$ and $CuSO_4$ treatments in the subventricular zone, the other established location of adult neurogenesis in mammals (Lois and Alvarez-Buylla, 1993). In addition, hippocampal neurogenesis rates decrease with age (Eriksson et al., 1998) but we did not observe a decrease in the number of autofluorescent cells in the hippocampi of older animals.

The source of the fluorescent signal described here is unclear. As previously described, autofluorescent signals generated by formaldehyde fixation and lipofuscin granules are effectively quenched by treating the sections with $NaBH_4$ and $CuSO_4$, respectively (Clancy and Cauller, 1998; Schnell et al., 1999). It is possible, however, that the population of cells remaining significantly autofluorescent after these treatments is a subpopulation of cells with high lipofuscin content. Lipofuscin accumulates with age as a result of oxidative stress, appearing first and accumulating fastest in the hippocampus (Oenzil et al., 1994). Qualitative assessments of the relative number of autofluorescent cells indicated that there was little or no correlation with the animal's age and, because most of the brains were obtained from animals that were 5–7 months old with only individual animals representing other age groups, quantitative assessment was not pursued. However, low numbers of autofluorescent cells in the youngest brain, in combination with all middle aged brains

showing autofluorescent cells, specifically in the hippocampus, support the conclusion that this signal may be derived from lipofuscin. In addition, the granular autofluorescence observed in somata in sections treated with both $NaBH_4$ and $CuSO_4$ is similar in distribution and appearance to other published descriptions of lipofuscin autofluorescence (Kwiatkowski et al., 2009; Monji et al., 1994; Oenzil et al., 1994; Schnell et al., 1999). Protocols for treatment with $CuSO_4$ must balance effective quenching of lipofuscin autofluorescence against attenuation of fluorophore activity and therefore may result in incomplete quenching of highly autofluorescent cells in hippocampus. On the other hand, autofluorescent signals seen evenly distributed in neurites are very different from the punctate pattern expected with lipofuscin autofluorescence and may derive from a different source.

An alternate source of autofluorescence is the neurotransmitter serotonin (5-HT). This molecule is abundant in the hippocampus and is characterized in fixed tissue by an emission spectrum with a main band at 440 nm and a shoulder around 510 nm in response to excitation at 366 nm (Crespi et al., 2004). Immunohistochemistry confirmed, however, that 5-HT expression is very widespread and does not correlate with distribution of autofluorescence in brain sections treated with $NaBH_4$ and $CuSO_4$. A third common source of autofluorescence in brain tissue at the relevant wavelengths is the reduced pyridine nucleotide, NADH (Chance et al., 1962), the synthesis of which can be imaged in real time using autofluorescence to monitor cellular activity in live tissues (Shuttleworth, 2009). The absorbance and emission spectra of NADH are quite broad around peaks at 340–360 nm and 430–450 nm respectively (Shuttleworth, 2009). Although fixing of tissues with formaldehyde alters the fluorescent properties of that tissue, NADH autofluorescence spectra are essentially unchanged by this process (Majumder et al., 2005). In fixed tissue, NADH emission is a broad band centered around 455 nm when illuminated with an N_2 (UV) laser (Majumder et al., 2005). In living tissues, NADH fluorescence depends on association of this coenzyme with complex I, which also extends the time of the fluorescence, and is therefore observed primarily inside the mitochondria while being quenched in the cytoplasm (Blinova et al., 2008; Chance and Baltscheffsky, 1958). Due to the importance of mitochondria in cellular life and function, they are regularly moved throughout a neuron via axonal transport mechanisms (Hollenbeck and Saxton, 2005). In fixed tissue at relatively low magnifications such as the ones used here, this would result in uniform fluorescence of the cytoplasm throughout the cell.

Due to its broad excitation and emission properties, NADH might be detected, albeit not at its peak excitation or emission, by the filter sets used here (recommended for eGFP). However, this molecule is broadly distributed in the brain and its localization to a select group of neurons is highly unlikely. It is possible that these particular cells have unusually high concentrations of NADH; perhaps they represent members of a circuit that was highly metabolically active at the time of fixing. It is more likely, however, that a different molecule or unique association of proteins, more specifically localized to a small subset of cells, is responsible for generating the observed autofluorescent signal.

Further studies to identify the source of the autofluorescent signal might include immunolabeling for candidate molecules such as complex I, and comparison of gene expression profiles of autofluorescent cells with those of their neighbors using single cell RT-PCR approaches. Detailed spectral analysis of the emission and excitation properties of the autofluorescent cells could identify potential sources of the fluorescent signal and test the hypothesis that the source is a type of lipofuscin.

Although identification of the molecule responsible for generating the autofluorescent signal described here will make an interesting goal for future studies, it is important that investigators be aware of the presence of this potential confound regardless of its source.

Unlike the generalized lipofuscin autofluorescence observed in the pyramidal cell layer of the hippocampus, the cells described here appear as individuals with strong autofluorescence in the soma and neurites that make them stand out from their neighbors and appear as distinct and unique. Investigators using GFP to track cells in the nervous system should control for the presence of these persistently autofluorescent cells that will result in false positives even in brains from young animals.

Acknowledgments

Lacey Hazel provided excellent technical support. We thank Dr. B. Antonsen for critical reading of the manuscript and insightful discussions. This work was supported by NSF EPS0554328, EPS1003907 and NIH HL084111.

References

Blandini F, Armentero MT, Martignoni E. The 6-hydroxydopamine model: news from the past. Parkinsonism Relat Disord. 2008; 14 (Suppl 2):S124–9. [PubMed: 18595767]

Blinova K, Levine RL, Boja ES, Griffiths GL, Shi ZD, Ruddy B, Balaban RS. Mitochondrial NADH fluorescence is enhanced by complex I binding. Biochemistry. 2008; 47:9636–45. [PubMed: 18702505]

Brederlau A, Correia AS, Anisimov SV, Elmi M, Paul G, Roybon L, Morizane A, Bergquist F, Riebe I, Nannmark U, Carta M, Hanse E, Takahashi J, Sasai Y, Funa K, Brundin P, Eriksson PS, Li JY. Transplantation of human embryonic stem cell-derived cells to a rat model of Parkinson's disease: effect of in vitro differentiation on graft survival and teratoma formation. Stem Cells. 2006; 24:1433–40. [PubMed: 16556709]

Chalfie M, Tu Y, Euskirchen G, Ward WW, Prasher DC. Green fluorescent protein as a marker for gene expression. Science. 1994; 263:802–5. [PubMed: 8303295]

Chance B, Baltscheffsky H. Respiratory enzymes in oxidative phosphorylation. VII. Binding of intramitochondrial reduced pyridine nucleotide. J Biol Chem. 1958; 233:736–9. [PubMed: 13575447]

Chance B, Cohen P, Jobsis F, Schoener B. Intracellular oxidation-reduction states in vivo. Science. 1962; 137:499–508. [PubMed: 13878016]

Clancy B, Cauller LJ. Reduction of background autofluorescence in brain sections following immersion in sodium borohydride. J Neurosci Methods. 1998; 83:97–102. [PubMed: 9765122]

Crespi F, Croce AC, Fiorani S, Masala B, Heidbreder C, Bottiroli G. Autofluorescence spectrofluorometry of central nervous system (CNS) neuromediators. Lasers Surg Med. 2004; 34:39–47. [PubMed: 14755423]

Eriksson PS, Perfilieva E, Bjork-Eriksson T, Alborn AM, Nordborg C, Peterson DA, Gage FH. Neurogenesis in the adult human hippocampus. Nat Med. 1998; 4:1313–7. [PubMed: 9809557]

Gage FH. Mammalian neural stem cells. Science. 2000; 287:1433–8. [PubMed: 10688783]

Hollenbeck PJ, Saxton WM. The axonal transport of mitochondria. J Cell Sci. 2005; 118:5411–9. [PubMed: 16306220]

Karlsson J, Petersen A, Gido G, Wieloch T, Brundin P. Combining neuroprotective treatment of embryonic nigral donor tissue with mild hypothermia of the graft recipient. Cell Transplant. 2005; 14:301–9. [PubMed: 16052911]

Kong Q, Wu M, Huan Y, Zhang L, Liu H, Bou G, Luo Y, Mu Y, Liu Z. Transgene expression is associated with copy number and cytomegalovirus promoter methylation in transgenic pigs. PLoS One. 2009; 4:e6679. [PubMed: 19688097]

Kwiatkowski TJ Jr, Bosco DA, Leclerc AL, Tamrazian E, Vanderburg CR, Russ C, Davis A, Gilchrist J, Kasarskis EJ, Munsat T, Valdmanis P, Rouleau GA, Hosler BA, Cortelli P, de Jong PJ, Yoshinaga Y, Haines JL, Pericak-Vance MA, Yan J, Ticozzi N, Siddique T, McKenna-Yasek D, Sapp PC, Horvitz HR, Landers JE, Brown RH Jr. Mutations in the FUS/TLS gene on chromosome 16 cause familial amyotrophic lateral sclerosis. Science. 2009; 323:1205–8. [PubMed: 19251627]

Lim ST, Airavaara M, Harvey BK. Viral vectors for neurotrophic factor delivery: a gene therapy approach for neurodegenerative diseases of the CNS. Pharmacol Res. 2010; 61:14–26. [PubMed: 19840853]

Lois C, Alvarez-Buylla A. Proliferating subventricular zone cells in the adult mammalian forebrain can differentiate into neurons and glia. Proc Natl Acad Sci U S A. 1993; 90:2074–7. [PubMed: 8446631]

Majumder SK, Ghosh N, Gupta PK. N2 laser excited autofluorescence spectroscopy of formalin-fixed human breast tissue. J Photochem Photobiol B. 2005; 81:33–42. [PubMed: 16107317]

Monji A, Morimoto N, Okuyama I, Yamashita N, Tashiro N. Effect of dietary vitamin E on lipofuscin accumulation with age in the rat brain. Brain Res. 1994; 634:62–8. [PubMed: 8156392]

Oenzil F, Kishikawa M, Mizuno T, Nakano M. Age-related accumulation of lipofuscin in three different regions of rat brain. Mech Ageing Dev. 1994; 76:157–63. [PubMed: 7885062]

Schnell SA, Staines WA, Wessendorf MW. Reduction of lipofuscin-like autofluorescence in fluorescently labeled tissue. J Histochem Cytochem. 1999; 47:719–30. [PubMed: 10330448]

Serakinci N, Keith WN. Therapeutic potential of adult stem cells. Eur J Cancer. 2006; 42:1243–6. [PubMed: 16678403]

Sharp J, Keirstead HS. Stem cell-based cell replacement strategies for the central nervous system. Neurosci Lett. 2009; 456:107–11. [PubMed: 19429144]

Shetty AK, Rao MS, Hattiangady B. Behavior of hippocampal stem/progenitor cells following grafting into the injured aged hippocampus. J Neurosci Res. 2008; 86:3062–74. [PubMed: 18618674]

Shuttleworth CW. Use of NAD(P)H and flavoprotein autofluorescence, transients to probe neuron and astrocyte responses to synaptic activation. Neurochem Int. 2009

Song H, Stevens CF, Gage FH. Astroglia induce neurogenesis from adult neural stem cells. Nature. 2002; 417:39–44. [PubMed: 11986659]

Ungerstedt U. 6-Hydroxy-dopamine induced degeneration of central monoamine neurons. Eur J Pharmacol. 1968; 5:107–10. [PubMed: 5718510]

van Praag H, Schinder AF, Christie BR, Toni N, Palmer TD, Gage FH. Functional neurogenesis in the adult hippocampus. Nature. 2002; 415:1030–4. [PubMed: 11875571]

Webber DJ, Bradbury EJ, McMahon SB, Minger SL. Transplanted neural progenitor cells survive and differentiate but achieve limited functional recovery in the lesioned adult rat spinal cord. Regen Med. 2007; 2:929–45. [PubMed: 18034631]

Yamasaki TR, Blurton-Jones M, Morrissette DA, Kitazawa M, Oddo S, LaFerla FM. Neural stem cells improve memory in an inducible mouse model of neuronal loss. J Neurosci. 2007; 27:11925–33. [PubMed: 17978032]

Zeng X, Cai J, Chen J, Luo Y, You ZB, Fotter E, Wang Y, Harvey B, Miura T, Backman C, Chen GJ, Rao MS, Freed WJ. Dopaminergic differentiation of human embryonic stem cells. Stem Cells. 2004; 22:925–40. [PubMed: 15536184]

Zietlow R, Lane EL, Dunnett SB, Rosser AE. Human stem cells for CNS repair. Cell Tissue Res. 2008; 331:301–22. [PubMed: 17901985]

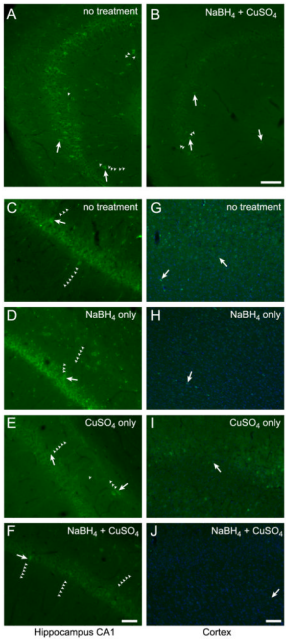

Figure 1.

Green autofluorescent cells are evident in hippocampus and cortex of rat brain sections after treatments to reduce endogenous fluorescence. Area CA3 of hippocampus in a brain section that was only washed and mounted (A). Same view of a serial section treated with $NaBH_4$ and $CuSO_4$ (B). CA1 of hippocampus (C–F) and cortex (G–J) in serial brain sections. Sections were either washed and mounted (C&G), treated with $NaBH_4$ only (D&H), treated with $CuSO_4$ only (E&I) or treated with both $NaBH_4$ and $CuSO_4$ (F&J). Arrows indicate examples of prominent autofluorescent cells and small arrowheads delineate autofluorescent cellular processes. A&B, C–F and G–J were identically acquired and adjusted for brightness for accurate comparison. Blue in G–J is TO-PRO-3 iodide staining of nuclei. Scale bars: A&B 100 μm, C–F 50 μm, G–J 100 μm.

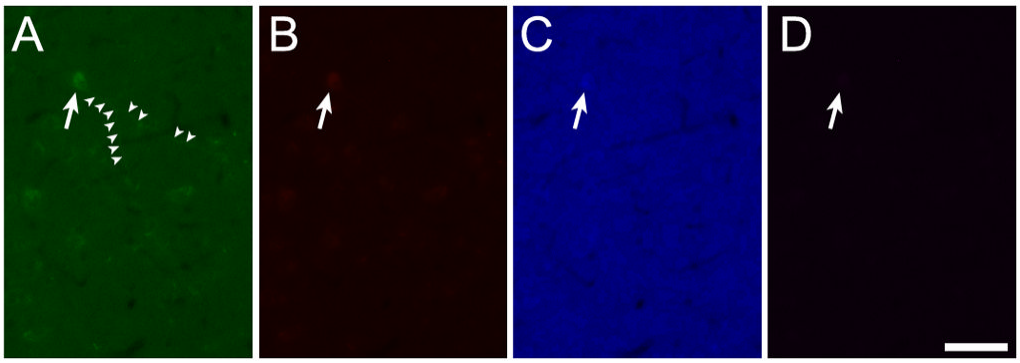

Figure 2.
Autofluorescent cells visible after chemical quenching fluoresce most strongly in the green channel (A) giving only weak signals in the red (B) and blue (C) channels and almost no signal at the far red (D) end of the spectrum. Scale bar: 50 μm.

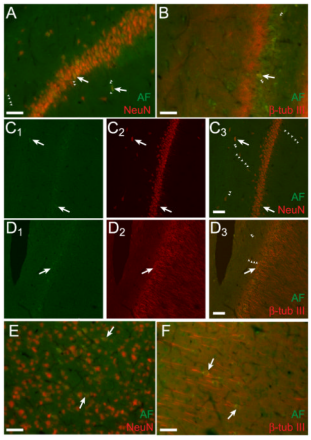

Figure 3.

Green autofluorescent cells in hippocampus and cortex represent a population of neurons. Green autofluorescent (AF) cells in area CA1 of hippocampus are immunopositive for NeuN (A) and β-tubulin III (B). Single optical slices (5 μm) of this area obtained with confocal microscopy confirm that the autofluorescent and immunofluorescent signals are localized to the same cells for NeuN (C) and β-tubulin III (D). For C and D, colors are separated for each slice with the left panels (green) showing autofluorescence (C_1&D_1), the middle panels (red) showing the immunolabel (red, C_2&D_2) and the right panels showing colocalization of the two signals in the same cells (merge, C_3&D_3). Epifluorescent micrographs of autofluorescent green cells in cortex labeled for NeuN (E) and β-tubulin III (F). Arrows indicate prominently autofluorescent immunopositive cells. Some autofluorescent cells are indicated with arrows and select autofluorescent cellular processes are delineated with small arrowheads. Scale bars: 50 μm.

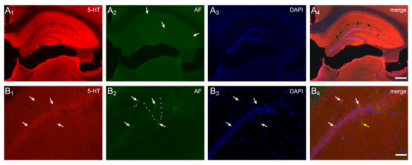

Figure 4.

Serotonin (5-HT) is not the source of the autofluorescent signal. Immunolabeling for 5-HT demonstrated that this biogenic amine is present in high levels throughout the hippocampus (A_1). Several green autofluorescent cells are visible in this section, some of these are indicated with arrows (A_2). DAPI staining of all nuclei in the section (A3). A merged image of all channels (A_4). Higher magnification of the pyramidal cell layer shows labeling for 5-HT in most somata and many fibers in the region (B_1). Several green autofluorescent cells are visible in this field (B_2, arrows), including cells with autofluorescent processes (small arrowheads). DAPI staining of nuclei (B_3). A merged image illustrates that some autofluorescent cells immunolabel for 5-HT (B_4, white arrows) while others do not (B_4, yellow arrow). Scale bars: A 500 μm, B 50 μm.

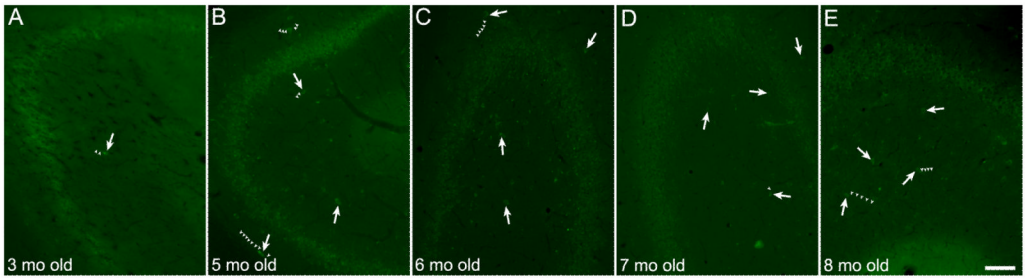

Figure 5.

Extent of hippocampal cellular autofluorescence does not correlate with age. Representative images of autofluorescent cells in the hippocampus in brains treated with $NaBH_4$ and $CuSO_4$ from animals of different ages as indicated in the bottom left corner of each panel. Some autofluorescent cells are indicated with arrows and select autofluorescent cellular processes are delineated with small arrowheads. Scale bar: 100 μm.

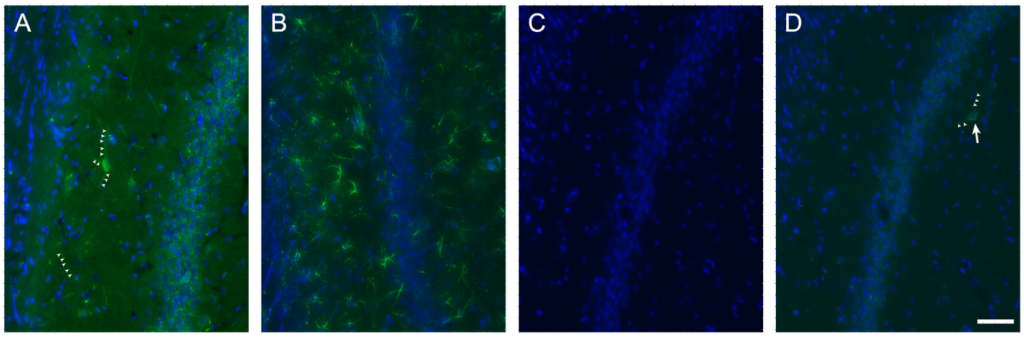

Figure 6.

Green autofluorescent cells are lost in the background when an immunofluorescent green signal is present. Autofluorescent green cells (arrows) with autofluorescent processes (small arrowheads) are prominent in hippocampus area CA1 (A) of untreated rat brain sections. A serial section treated with $NaBH_4$, $CuSO_4$ and a green antibody against GFAP (B) shows that the immunohistochemical green signal is significantly brighter than the endogenous autofluorescence, rendering the autofluorescent cells invisible. A serial section processed as B but omitting the primary antibody and exposed for the same time as B has no visible green cells (C). The same field exposed for a longer time (D) reveals an autofluorescent cell (arrow). Exposure times on green channel: A&D 384 ms, B&C 93 ms. Blue in all panels is nuclei labeled with DAPI. Scale bar: 50 μm.

Table 1

Summary of rat brains evaluated in this study.

A total of 20 rat brains from animals ranging in age from 3 to 9 months were evaluated in this study. Some animals were completely naïve while others had received a unilateral 6-OHDA lesion to the medial forebrain bundle, a common model for Parkinson's disease. One animal received a sham (saline) injection to the striatum on the lesioned side following the 6-OHDA lesion as part of a cell transplant study. No animals were exposed to GFP or other fluorescent molecules. The relative number or autofluorescent (AF) cells observed in each brain are indicated with (+) indicating few cells and (+++) representing high numbers of autofluorescent cells. For animals that had received treatments, only the contralateral side of the brain was evaluated for the presence of autofluorescent cells. The right column indicates figures that show representative images for individual animals

Rat	Age (months)	Treatments	Relative number AF cells	Shown in Figure:
1	3	None	+	5A
2	4	Contralateral 6-OHDA lesion only	+++	1AB, 3, 4B
3	5	None	++	
4	5	None	+++	
5	5	None	++	
6	5	None	++	5B
7	6	None	+	
8	6	Contralateral 6-OHDA lesion only	+++	
9	6	Contralateral 6-OHDA lesion only	++	5C
10	6	Contralateral 6-OHDA lesion only	++	
11	6	Contralateral 6-OHDA lesion only	+	
12	6	Contralateral 6-OHDA lesion only	++	
13	7	Contralateral 6-OHDA lesion only	++	6
14	7	Contralateral 6-OHDA lesion only	+++	1C–F, 4A
15	7	Contralateral 6-OHDA lesion only	+	
16	7	Contralateral 6-OHDA lesion only	+	1G–J, 5D, 2
17	7	Contralateral 6-OHDA lesion only	+++	
18	7	Contralateral 6-OHDA lesion only	++	
19	8	None	++	5E
20	9	Contralateral 6-OHDA lesion and sham injection	++	